Phase Behavior of an Ionic Surfactant with Mixed Monovalent/Polymeric Counterions†

Anna Svensson,[#] Lennart Piculell,*[,#] Lisa Karlsson,[#] Bernard Cabane,[‡] and Bo Jönsson[§]

Physical Chemistry 1 and Theoretical Chemistry, Center for Chemistry and Chemical Engineering, Lund University, P.O. Box 124, S-221 00 Lund, Sweden, and Laboratoire PMMH, ESPCI, 10 rue Vauquelin, 75231 Paris Cedex 05, France

Received: October 22, 2002; In Final Form: April 9, 2003

A "complex salt" of cetyltrimethylammonium (CTA^+) with short (30 repeating units) polyacrylate (PA^-) counterions has been synthesized. The phase diagrams of its aqueous mixtures with either the surfactant cetyltrimethylammonium acetate (CTAAc), or the polyelectrolyte NaPA, have been studied by visual inspection through crossed polarizers and by small-angle X-ray scattering. Both of the ternary phase diagrams are strikingly simple, containing only micellar, cubic micellar, and hexagonal phases. In the CTAPA/CTAAc/water system, the surfactant forms essentially spherical micelles above ca. 50 wt % of water, regardless of the counterion composition, and the system may serve as a model for charged colloids with mixed monovalent/polymeric counterions. The interactions between micelles varies from repulsive to attractive as the fraction of monovalent counterions is decreased. This results, first, in a liquid−liquid phase separation between a concentrated branch and a dilute branch of the micellar phase and, finally, a crystallization of micelles into a cubic ($Pm3n$) phase in equilibrium with essentially pure water. Small fractions of polymeric counterions "melt" the cubic phase. This is attributed to heterogeneity: A small proportion of micelle pairs that share polymeric counterions experience strong attractions. In CTAPA/NaPA/water mixtures, the micelle−micelle interactions switch from attractive to repulsive as the NaPA content is increased. A similar effect occurs with added NaAc. Monte Carlo simulations of interactions between surfactant aggregates neutralized by mixed polymeric and monovalent counterions qualitatively reproduce all experimental trends and show that the dominating source of the attraction between the aggregates is polyion bridging.

Introduction

Mixtures of polymers and surfactants are found in many applications and constitute an extensively studied research subject.[1,2] For oppositely charged species, a common behavior in water solutions is an association of the oppositely charged polyions and surfactant ions into a concentrated phase. This can be observed as a precipitation in an aqueous solution,[3−8] a deposition on a surface,[9,10] or a collapse of a polyelectrolyte gel in a surfactant solution.[11−17] Recently, interest has been focused on the structures and compositions of these concentrated phases.[18−28] Many researchers tend to approach these systems from a "polymer-centered" viewpoint, asking how the small surfactant ions interact with a matrix of large polyions.[29] However, it is, by now, well established that polymer/surfactant mixtures generally contain surfactant *aggregates*, similar to those found in the simpler mixtures of ordinary surfactants (containing only simple monovalent counterions) and water. Thus, it seems warranted to adopt a "surfactant-centered" viewpoint, from which the following questions regarding concentrated polyion-surfactant systems emerge naturally. How do polymeric counterions, or mixed polymeric/simple counterions, influence the shape and aggregation number of the surfactant aggregate? What determines the water solubility of such aggregates? What type of structures (disordered micellar or liquid crystalline) do the aggregates form in concentrated systems? How are the aggregates and phases related to those formed by ordinary surfactants in water?

The conventional strategy when investigating the phase behavior of oppositely charged systems is to mix a *polyelectrolyte* (polyion + simple counterion) with a *surfactant* (surfactant ion + simple counterion). However, the compositions of the phases that separate out from such a mixture may generally not be described in terms of combinations of polyelectrolyte and surfactant, because the ions tend to pair in an alternative way: as a *complex salt* (polyion + surfactant ion) and as a *simple salt* (a combination of the simple ions). Clearly, a complete description of the phase behavior of this four-component system must allow for all possible combinations of the four ions that do not violate the condition of macroscopic electroneutrality. One such description, proposed by Thalberg et al., can be described in terms of a tetragonal pyramid (see Figure 1).[7] The figure shows how the conventional mixtures of polyelectrolyte and surfactant in water represent a plane—the "conventional mixing plane"—in the pyramid. Moreover, the figure illustrates that the compositions of two separating phases are not located within the mixing plane.

Recently, we introduced a new approach to the phase studies of oppositely charged polymer−surfactant mixtures.[26] The essence of the approach is to reduce the number of components in the mixture by synthesizing the pure complex salt (Figure 2a) and using it as one of the starting components of the mixtures. The complex salt is a natural point of departure, because it represents a strongly preferred pairing of the ions present in the mixture. The complex salt is then mixed with

† Part of the special issue "International Symposium on Polyelectrolytes".

* Author to whom correspondence should be addressed. E-mail: Lennart.Piculell@fkem1.lu.se.

[#] Physical Chemistry 1, Lund University.

[‡] ESPCI.

[§] Theoretical Chemistry, Lund University.

10.1021/jp027275g CCC: $25.00
Published on Web 05/24/2003

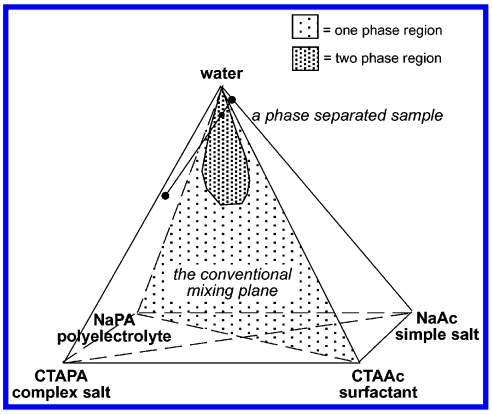

Figure 1. Three-dimensional pyramid phase diagram (schematic) that fully describes the phase behavior of aqueous mixtures of a charged surfactant with an oppositely charged polyelectrolyte. See text for details.

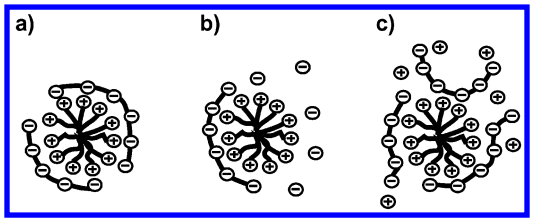

Figure 2. Schematic diagrams showing (a) the complex salt; (b) the surfactant ion mixing plane, which contains surfactant aggregates with mixed simple/polymeric counterions; and (c) the polyion mixing plan, which contains polyions with mixed simple/surfactant counterions.

either surfactant or polyelectrolyte. Each of these mixtures contains only three ionic species, plus water, and thus represents a truly ternary mixture, corresponding to one of the faces of the pyramid in Figure 1. Mixtures of the complex salt and surfactant in water will thus contain surfactant ions with mixed polymeric and monovalent counterions (see Figure 2b). These mixtures are represented by the front face of the pyramid in Figure 1, and we will refer to this plane as the *surfactant ion mixing plane*. Conversely, mixtures containing the complex salt and polyelectrolyte in water will contain polyions with mixed simple and surfactant counterions (see Figure 2c). Such mixtures are described by the left-hand face of the pyramid, which we call *the polyion mixing plane*.

In our initial study using the aforementioned strategy, we investigated a surfactant ion mixing plane.[26] The complex salt was cetyltrimethylammonium polyacrylate (CTAPA), with a short polyacrylate as the polymeric counterion. The surfactant was cetyltrimethylammonium bromide (CTABr). The resulting phase diagram is shown in Figure 3. The choice of system was based on the earlier work performed in our laboratories, where we studied conventional mixtures of a short sodium polyacrylate (NaPA) and CTABr.[5,22] The use of the alternative strategy, on the basis of the complex salt, resulted in several important conclusions on the phase behavior of the system:

(1) The phase diagram of Figure 3 contains all those phases that had previously been found to separate out from conventional NaPA/CTABr mixtures, and it shows how these phases are related.[5,22] For instance, it is clear from Figure 3 why the most commonly observed strucure that separates out from NaPA/CTABr mixtures is a hexagonal phase, where the proportions of bromide and polyacrylate counterions may vary within wide ranges.[22] It is also clear that this phase is connected to the normal hexagonal phase of pure CTABr in water.

(2) The properties of binary mixtures of complex salt and water are elucidated. The complex salt CTAPA is water-

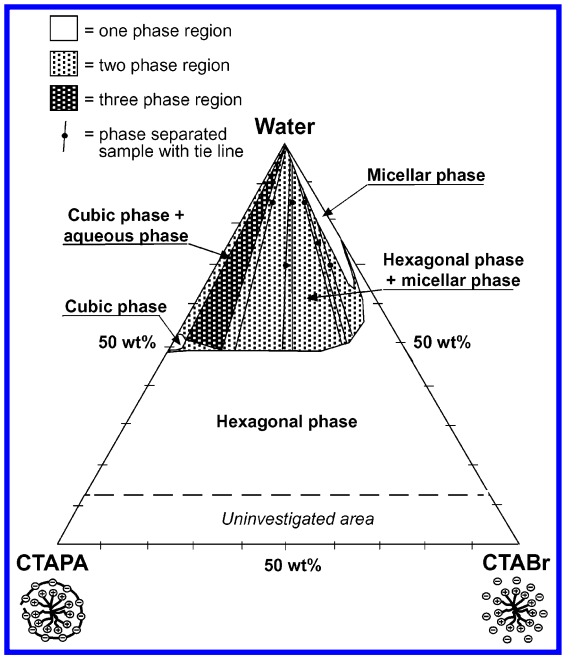

Figure 3. Experimental surfactant ion phase diagram of the complex salt CTAPA, the surfactant CTABr, and water at 40°C.

insoluble, but it can absorb substantial amounts of water, forming first a hexagonal phase and, at higher water contents, a micellar cubic phase (*Pm*3*n*). The maximum water uptake of the cubic phase is reached at ca. 55 wt % of water. A sample containing more water forms a cubic phase in equilibrium with almost-pure water.

(4) The results show that the shape of the surfactant aggregates is determined by the nature of the counterion. The cubic phase is destroyed by a small fraction of bromide counterions. This is because bromide counterions, as is well documented, shield the surfactant headgroup repulsion more efficiently than ions such as chloride or acetate.[22,30,31] This results here in a growth of cationic surfactant aggregates, from small micelles to extended cylinders.

In this study, we continue our experimental investigation of ternary mixtures based on CTAPA, with two major aims in mind:

(1) To study a surfactant ion plane containing a simple surfactant counterion that does not give rise to micellar growth. The isolated effect of "polymerizing the counterion" then can be studied for surfactant aggregates with a constant shape.

(2) To study the polyion mixing plane, i.e., mixtures of CTAPA, NaPA, and water.

As the alternative simple ion, we have chosen acetate, which contains the same charged group—the carboxylate group—as polyacrylate. Cetyltrimethylammonium acetate (CTAAc) gives spherical micelles in water and forms a micellar cubic phase at high concentrations.[22]

To obtain a better understanding of the interactions giving rise to the experimental phase diagrams, we have also performed Monte Carlo simulations of model surfactant aggregates. Simulations were performed for both the surfactant ion and the polyion mixing planes.

Materials and Methods

Materials. Poly(acrylic) acid (HPA) with an average molar mass of 2000 g/mol was purchased from Aldrich. The HPA is the same product, but not the same batch, as that used in the research of Ilekti and co-workers.[5,22] The latter batch was

examined by size-exclusion chromatography, coupled with low-angle light scattering, giving a number-average molar mass (M_n) of 2800 g/mol and a weight-average mass (M_w) of 4700 g/mol.[5]

The HPA was purified by dialysis for 5 days against Millipore water, followed by freeze drying. ^{1}H NMR revealed a small amount of structural impurity, which remained unchanged in intensity after the dialysis procedure. Two different batches of HPA both showed the presence of the impurity, which we tentatively ascribe to heterounits at the ends of the short polymer, originating from a termination reaction in the synthesis procedure. Titration with NaOH showed that the equivalent molar mass of the HPA was 89.3 g/(mol carboxylic acid), as compared to the theoretical value of 72 g/mol. Presumably, this difference is due primarily to the heterounits in the polymer. The contribution from water to the equivalent molar mass should be small: The water uptake of freeze-dried HPA exposed to ambient air was found to be 2 wt % after 1 h and 5 wt % after several days.

CTABr was purchased from Merck and used without further purification. The molar mass of CTABr is 364.5 g/mol. CTAPA was prepared by titrating the hydroxide form of the surfactant with the acid form of the polymer. The first step was to convert CTABr to CTAOH by ion exchange.[32] The ion-exchange resin (Dowex SBR, dry mesh 20−50, from Sigma) was charged by stirring in an excess amount of 1 M NaOH for 2 h and then rinsed with Millipore water until the rinsing water reached pH 7. CTABr (30 g) was then dissolved in a plastic beaker that contained a large excess (200 g) of the charged ion-exchange resin and 250 mL of Millipore water. The solution was stirred until all the CTABr was dissolved. The slurry was filtered, and the filtrate was rinsed with Millipore water into a fresh batch of 200 g of resin and 250 mL of water, which was stirred for another 2 h. The last step was repeated once. The alkaline solution now contained CTAOH at a concentration of ∼0.05 M. A 0.5 M solution of HPA was titrated drop by drop into the freshly prepared solution of CTAOH, under stirring. This was done immediately, to avoid Hofmann elimination of the quaternary ammonium hydroxide group of the surfactant in the basic solution.[33] The pH was measured with a standard pH electrode. A white precipitate, the complex salt, was formed at the start of the titration, which was continued until the equivalence point was reached. The latter point was taken as the inflection point (pH 8.6) in the pH titration curve, determined in a separate measurement. After the solution was equilibrated overnight, the solution with the precipitate was freeze-dried. The complex salt was then obtained as a white, hygroscopic powder, which was put into storage over a silica gel in a desiccator. Titrimetric analysis gave a bromide content below the detection limit (0.3 wt %) in the complexes. CTAAc was prepared by the same procedure, i.e., by titrating CTAOH with acetic acid to the equivalence point (pH 8.1). The resulting CTAAc solution was clear. After the solution was freeze-dried, CTAAc was obtained as a white powder and put into storage over a silica gel in a desiccator. Sodium polyacrylate (NaPA) was prepared by titrating the poly(acrylic acid) with NaOH to the equivalence point (pH 8.6), followed by freeze-drying.

Weighing experiments indicated a weight increase of both CTAPA and CTAAc, through water uptake, by ∼10 wt % in the desiccator, and by 20 wt % after prolonged storage in air. The water uptake of the polyelectrolyte NaPA was also 10 wt % in the desiccator, but ∼50 wt % after prolonged storage in air. Care was taken to minimize the exposure of the components to air during sample preparation. A water content of 10 wt % in CTAPA, CTAAc, and NaPA was assumed when calculating the sample compositions.

The fraction of acetate counterions in a sample in the surfactant ion mixing plane will be expressed in terms of equivalent charge as

$$x_{Ac} = \frac{\text{equivalents of acetate}}{\text{equivalents of acetate} + \text{acrylate}} \quad (1)$$

The experimentally determined equivalent molar mass of polyacrylate (cf. above) was used when calculating x_{Ac}.

Sample Preparation. Appropriate amounts of complex salt, surfactant (or polyelectrolyte), and water were weighed and put in glass tubes. After the compounds were mixed together with a Vortex vibrator, the tubes were flame-sealed. The mixing was continued in a centrifuge during 6 h at 4000 rpm and 40 °C. The tubes were turned end over end every 15 min. The samples were left to equilibrate at 25 °C for several weeks.

Structures and Compositions of Equilibrium Phases. All samples were investigated by visual inspection in normal light and between crossed polarizers to detect optically anisotropic phases (in the present case, the hexagonal phase). Small-angle X-ray scattering (SAXS) measurements were performed with two different setups. At the D 43 instrument at the LURE facility in Orsay, France, a parallel monochromatic beam with a wavelength of 1.445 Å was focused with point collimation on the sample. The sample was contained in a flat cell with mica windows and kept at 25 °C. The sample-to-detector distance was 377 mm. A Kratky compact small-angle system with linear collimation was used at the Lund laboratory. The X-rays were detected with a position-sensitive detector. The wavelength was 1.54 Å, and the sample-to-detector distance was 277 mm. The sample cell had mica windows and was maintained at 25 °C.

The water contents of the coexisting micellar phases in the surfactant ion mixing plane were determined by thermal gravimetric analysis (TGA).

Computational Methods. Metropolis Monte Carlo simulations[34] were performed for spherical and planar aggregate geometries, on the basis of a dielectric continuum model for the electrostatic interactions. The cell model was used for spherical micelles, with a charged micelle at the center of the cell. The neutralizing counterions, and possible excess ions, were allowed to sample the volume between the micellar surface and the cell boundary. The cell radius was chosen so as to describe the surfactant concentration. The micelle radius was estimated to be 24 Å, corresponding to a stretched hydrocarbon chain in the CTA^+ ion. The aggregation number was 94, giving a uniform surface charge density of 0.13 C/m^2.

The polyacrylate ions were modeled as charged hard spheres, with a radius of 2 Å, connected by simple harmonic bonds to decamers with an average charge−charge separation of 5 Å. Extensive simulations have shown that the length of the polyion is of minor importance after it is larger than a few monomers.[35] This was confirmed in the present study by selected calculations for polyions containing 30 charged units. The average monomer−monomer separation affects the forces in a quantitative, but not qualitative, way.

The cell model is eminently suited for studies of a single micelle with simple counterions. In systems where one can expect that the interaction between micelles is modulated by bridging polyions, it becomes less applicable. To include more than one micelle in a spherical cell is possible, but such an approach is limited to high water contents, unless the number of micelles per cell is made large. Another alternative, which we have used here, is to calculate the free energy of interaction

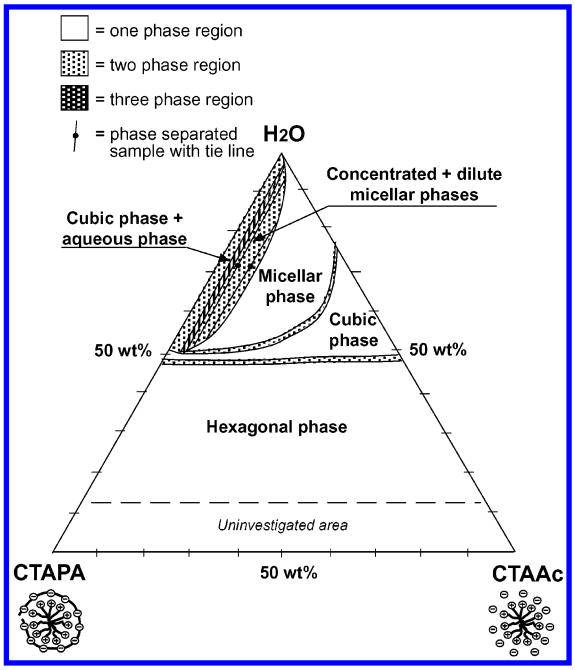

Figure 4. Experimental surfactant ion phase diagram of the complex salt CTAPA, the surfactant CTAAc, and water at 25°C.

per unit area between two infinite charged planes, A_{planes}, and then obtain the force between two identical spheres, $F_{spheres}$, by applying the Derjaguin approximation[36]

$$F_{spheres}(h) = \pi R A_{planes}(h) \qquad (2)$$

Here, h is the (shortest) distance between the surfaces and R is the radius of the spheres.

The force between two charged planar surfaces is obtained from the simulations via a modified form of the so-called contact theorem.[35] The free energy of interaction, A_{planes}, is then obtained by numerical intergration of the simulated pressure−distance curve.

Results

The Surfactant Ion Plane. A ternary phase diagram of mixtures of CTAPA, CTAAc, and water, based on more than 80 samples, is shown in Figure 4. Before describing the diagram and the various phases it contains in some detail, we note that the phase diagram is strikingly simple, and that it is significantly different from the diagram in Figure 3. Figure 4 contains three one-phase regions, where two (the cubic and the hexagonal) extend across all counterion compositions, and one (the micellar) extends almost completely across all compositions. In addition, there are four biphasic regions and one three-phase triangle.

The Binary Mixtures. The binary mixtures, which are represented by the left and the right axes of the phase triangle, both conformed to the behavior observed previously for CTAPA/water[26] (see the Introduction) and CTAAc/water[22] mixtures, respectively. Figure 5a shows the SAXS spectrum of the cubic (*Pm*3*n*) phase of CTAPA/H_2O. This phase can coexist with almost-pure water. The phase boundary between the cubic phase and the two-phase coexistence region was difficult to locate exactly. Biphasic samples close to the phase boundary did not readily phase-separate macroscopically. When the volume of the water phase was small, it remained dispersed throughout the cubic phase, because of the solidlike texture of the latter. As the water content was increased, biphasic samples

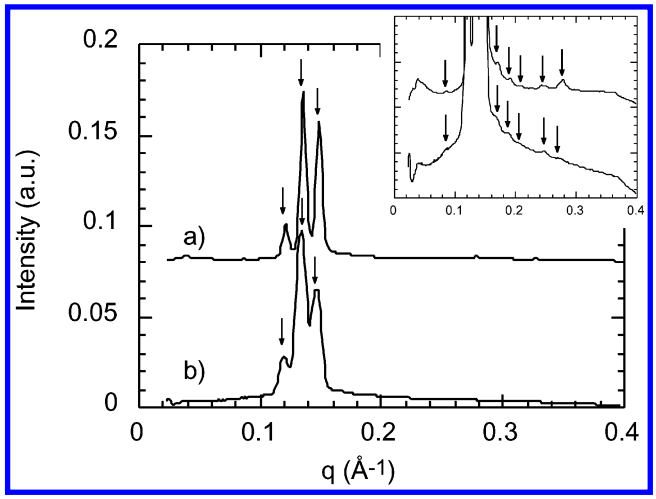

Figure 5. SAXS spectra of cubic *Pm*3*n* samples at 25°C for two binary mixtures containing 55 wt % water and (a) 45 wt % CTAPA or (b) 45 wt % CTAAc. Relative locations of peaks (with invisible peaks of the *Pm*3*n* structure given in parentheses): (1), $2^{1/2}$, $4^{1/2}$, $5^{1/2}$, $6^{1/2}$, $8^{1/2}$, $10^{1/2}$, $12^{1/2}$, ($13^{1/2}$), $14^{1/2}$, $16^{1/2}$, $17^{1/2}$, ($18^{1/2}$), $20^{1/2}$, $21^{1/2}$. The peaks at $14^{1/2}$, $17^{1/2}$, and $21^{1/2}$ were not detected in these samples.

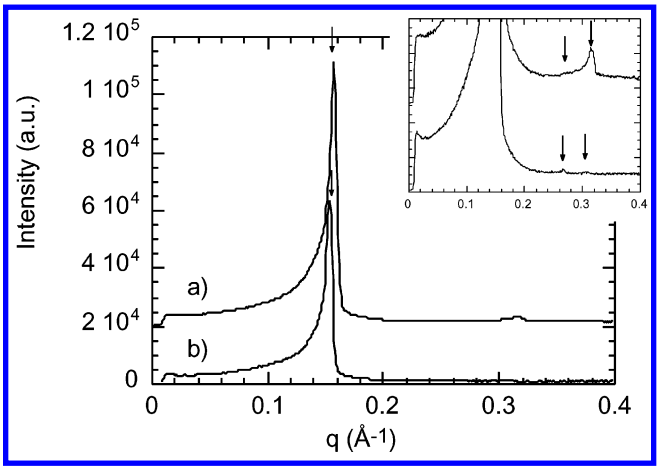

Figure 6. SAXS spectra of hexagonal samples at 25°C for two binary mixtures containing (a) 40 wt % water and 60 wt % CTAPA or (b) 41 wt % water and 59 wt % CTAAc. Relative locations of peaks: 1, $3^{1/2}$, $4^{1/2}$.

became increasingly turbid, until a macroscopic phase separation was finally observed. The onset of this increase in turbidity occurred in the range of 50−55 wt % of water, which is where we have drawn the phase border.

A narrow transition between the cubic and hexagonal phases occurred at lower water contents (45−50 wt %). The SAXS spectrum of a hexagonal sample containing 60 wt % CTAPA is shown in Figure 6a.

The binary CTAAc/water mixtures followed the typical phase sequence for a surfactant that does not display substantial micellar growth: A micellar phase was followed by a cubic phase and then a hexagonal phase, with increasing surfactant concentration. The micellar phase was clear, and its viscosity increased as the surfactant concentration increased. At ca. 25 wt % of surfactant, the phase transition from micellar to cubic phase took place. The cubic phase was hard, clear, and optically isotropic. Its structure was again of the *Pm*3*n* type, which has discrete surfactant micelles packed in a cubic array (see the SAXS spectrum in Figure 5b).[37] The hexagonal phase appeared at ca. 50 wt % of surfactant. The SAXS spectrum for a hexagonal sample containing 59 wt % CTAAc in water can be seen in Figure 6b.

TABLE 1: Aggregates and Structures in the Liquid Crystalline Phases of the Binary Mixtures CTAAc/H_2O and CTAPA/H_2O

	Cubic, *Pm*3*n*, 55 wt % Water		Hexagonal, 40 wt % Water	
	unit-cell dimension (Å)	micelle aggregation number, N_{agg}[a]	radius of hydrocarbon core, R_{agg}[b] (Å)	mean distance between centers of neighboring cylinders, $r_{center-center}$ (Å)
CTAAc	105	114	17.0	46.8
CTAPA	101	94	16.1	45.9

[a] Calculated as the number concentration of surfactant ions (obtained assuming a density of 1 g/cm^3 for the samples) divided by the number concentration of micelles (obtained from the unit-cell dimensions with eight micelles per unit cell). [b] Radius of the hydrocarbon core of a cylindrical aggregate; calculated from the unit-cell dimension and the volume fraction of surfactant chains, assuming infinite cylinders, a density of 1 g/cm^3 for the sample, and a volume of 459 Å^3 per hydrocarbon chain.

Clearly, the two pure counterion forms of the surfactant, CTAAc and CTAPA, give rise to the same aggregate types in their respective mixtures with water. At low water contents, hexagonal structures are formed. At ~50 wt % water, the aggregates are broken up into small micelles and arranged in a cubic phase of the *Pm*3*n* type. The similarities are further illustrated by Table 1, which gives data on aggregate dimensions and aggregate distances for the two pure counterion forms, calculated from the data in Figures 5 and 6. The micelles have an aggregation number (N_{agg}) that is close to the theoretical value of 95, calculated by Tanford's formula for a spherical micelle with cetyl chains.[38] The radius of the hydrocarbon core of a cylindrical aggregate in the hexagonal phase (R_{agg}) is somewhat shorter than the length of a fully stretched cetyl chain (22 Å). The main difference between micelles with polymeric and monovalent counterions appear at higher water contents: Micelles with monovalent counterions are completely miscible with water, whereas micelles with polymeric counterions remain insoluble as a cubic phase.

We will now turn our attention to samples with mixed polymeric and monovalent counterions, starting with the most concentrated mixtures in Figure 4 and then moving upward, in the direction of increasing water content.

The Hexagonal One-Phase Region. The hexagonal phase extends across the CTAPA/CTAAc/H_2O phase diagram and over a wide range of surfactant concentrations (see Figure 4). Figure 6 shows that the position of the first peak of the SAXS spectrum changes only slightly, from 0.155 Å^{-1} for pure CTAAc to 0.158 Å^{-1} for pure CTAPA. An intermediate peak position was found in a sample with mixed counterions at the same water content (not shown). Neither the maximum water content nor the structure of the hexagonal phase was affected by the counterion composition of the surfactant aggregates. Note that the molar mass per ion pair differs by only 8% between CTAPA and CTAAc. Therefore, the molar concentration of surfactant ions in a sample at a given water content is approximately independent of the counterion composition.

The Cubic/Hexagonal Two-Phase Region. At a water content slightly below 50 wt %, the hexagonal phase ends and the cubic *Pm*3*n* phase begins. The two phases coexist in a narrow region, which stretches as a belt horizontally across the phase diagram. Two samples were located inside the two-phase area and contained macroscopically separated hexagonal and cubic phases. The hexagonal phase collected in the top of the sample vial and showed bright birefringence between crossed polarizers. The cubic phase was nonbirefringent and was located in the bottom of the vial. This layering of the phases is in agreement with previous studies, which showed that the density (mass per unit volume) of CTAPA/water mixtures increases as the water content increases.[26]

The Cubic One-Phase Region. Similar to the hexagonal phase, the cubic *Pm*3*n* phase extends across the CTAPA/CTAAc/H_2O phase diagram. Unlike the hexagonal phase, however, the cubic phase varies strongly in its extension toward the water corner as the counterion composition is changed. The cubic phase of pure CTAAc/water (i.e., $x_{Ac} = 1$) can contain 50−75 wt % water. As the fraction of polyacrylate counterions is increased ($x_{Ac} < 1$), the maximum water content of the cubic phase decreases, initially quite rapidly. The cubic phase region becomes a very narrow band at high polyacrylate contents.

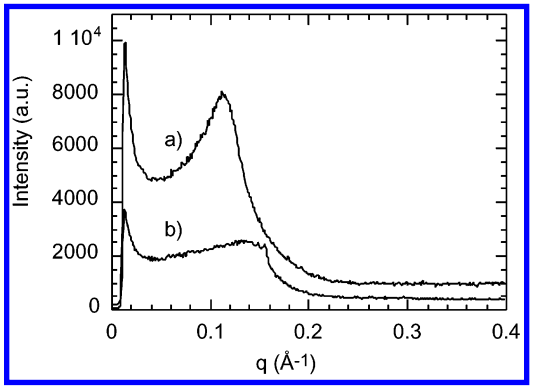

Figure 7. SAXS spectra of micellar samples at 73 wt % water in the CTAPA/CTAAc/water system with (a) $x_{Ac} = 0.85$ or (b) $x_{Ac} = 0.44$.

The Micellar One-Phase Region. Except at very high contents of polymeric counterions, the cubic phase is transformed to a micellar phase, via a narrow two-phase region, as the water content is increased. At sufficiently high contents of CTAPA, the micellar phase forms already at water contents almost as low as 50 wt %. The maximum fraction of polyacrylate counterions that the micellar phase may contain decreases as the water content increases. The most concentrated micellar samples have >80% polymeric counterions. SAXS data (Figure 7) reveal a strong and systematic broadening of the peak as the fraction of polyacrylate counterions is increased. This observation indicates strong concentration fluctuations; the micelles have a tendency to associate in clusters with a shorter intermicellar distance, presumably because they are bridged by the polyions. At a fixed water content, the viscosity of micellar samples increases as the content of polyacrylate increases.

The Micellar/Micellar Two-Phase Region. A region of coexistence between a concentrated branch and a dilute branch of the micellar phase was found at high contents of polyacrylate counterions. Samples in this region phase-separated macroscopically into two isotropic phases. Samples close to the boundary of the micellar one-phase region were initially turbid dispersions, and a long centrifugation (12 h) was required to achieve a macroscopic separation between the two clear phases. Deeper inside the two-phase region ($x_{Ac} < 0.2$), the samples separated spontaneously into a turbid, concentrated micellar phase on top of a clear and dilute micellar phase. After 6 h of centrifugation, the top phase also became clear. The difference in water content between the separated phases increased as the content of polyacrylate counterions increased. A critical point must exist somewhere along the phase boundary; however, its exact

TABLE 2: Water Content of the Micellar Phases in the Two-Phase Micellar Region, As Determined by TGA

wt % in sample CTAPA/CTAAc/H_2O	wt % water in concentrated phase	wt % water in dilute phase
15/5/80		94
20/10/70	63	82
25/5/70	55	97
35/10/55	49	

location was difficult to determine experimentally, because of the high viscosity of the samples. The tie lines drawn in Figure 4 are based on measurements of the water contents of the separated micellar phases (see Table 2).

The Cubic/Aqueous Two-Phase Region. At very high contents of polyacrylate, the micellar phase disappears. Samples with a water content of >50 wt % and with $x_{Ac} < 0.1$ contain the cubic phase in equilibrium with an aqueous phase. The cubic phase was initially turbid; however, in some two-phase samples, it became translucent after prolonged storage (several months) at 25 °C.

The Three-Phase Region. A three-phase triangle must be located between the micellar−micellar and the micellar−cubic two-phase areas. Indeed, we found two samples in this region that contained three layered phases: one hard, cubic phase on top of one translucid micellar phase and, at the bottom of the tube, one clear dilute phase.

The Polyion Mixing Plane. The CTAPA/NaPA/H_2O phase diagram is shown in Figure 8. The diagram is based on 60 samples and contains three single-phase regions, five two-phase regions, and two three-phase regions. We will approach this phase diagram by describing how aqueous mixtures, initially containing only complex salt and water, respond when increasing amounts of excess polyelectrolyte are added. The major effects of added polyelectrolyte are that the miscibility with water rapidly increases and the cubic phase disappears. Hence, the phase diagram is dominated by a large micellar phase and a large hexagonal phase.

The cubic phase can contain a maximum of 10 wt % NaPA; at higher contents of polyelectrolyte, it "melts" into a micellar phase. At a polyelectrolyte content above ca. 15 wt %, only micellar and hexagonal phases exist. These phases coexist in a relatively narrow two-phase area that, in the investigated composition range, extends in the direction toward the NaPA corner. This means that, when NaPA is added to coexisting hexagonal and micellar phases, it distributes equally between the two phases, without affecting the ratio between complex salt and water in either phase. Because added NaPA eventually resides in the aqueous subphase that separates the surfactant aggregates, it follows that both the hexagonal and the micellar phases can swell with added NaPA, in the sense that the distance between the surfactant aggregates becomes larger.

When NaPA is added to biphasic samples of cubic aqueous complex salt and water, the same phase sequence appears as when CTAAc is added to the same system. Small additions of NaPA lead to the appearance of a concentrated micellar phase that, after a narrow region of three-phase coexistence, replaces the cubic phase. As the NaPA content is increased further, the two coexisting micellar phases approach each other in composition, and, finally, they merge at a NaPA content of <10 wt %. Evidently, added polyelectrolyte increases the solubility of the complex salt. Excess simple salt has a similar effect;[5,7,12,14] therefore, we decided to make quantitative comparisons with the effect of added sodium acetate, NaAc. A solution of 30 wt % NaAc was added dropwise to a solution of 30 wt % CTAPA. Initially, the appearance of the phase-separated sample changed little as salt was added. At 7 wt % NaAc, however, two clear liquid phases were formed, indicating the coexistence of two micellar phases. At 9 wt % NaAc, a single clear solution appeared. This is quite close to the concentration of NaPA at the corresponding position on the phase boundary in Figure 8. Thus, when comparing the effects of added NaPA or NaAc, we found that the effects were quite similar, even quantitatively. The polyelectrolyte is approximately as efficient as the simple salt in dissolving the complex salt.

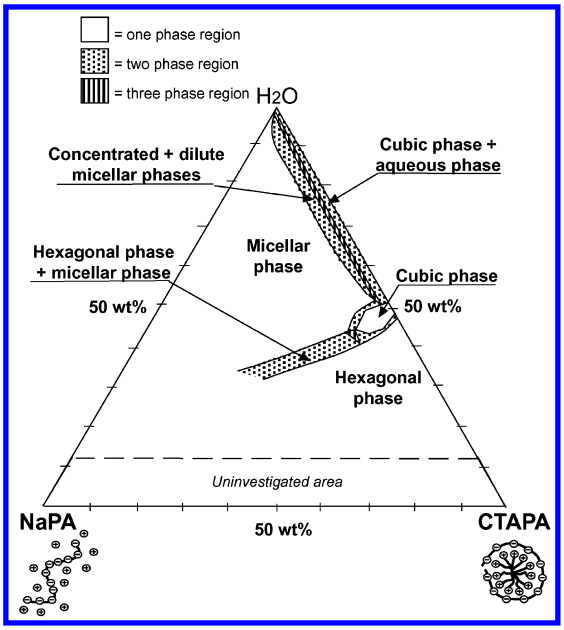

Figure 8. Experimental polyion phase diagram of the complex salt CTAPA, the polyelectrolyte NaPA, and water at 25°C.

Temperature Effects. The phase diagrams in Figures 4 and 8 were obtained at 25°C. The diagram in Figure 3, on the other hand, was investigated at 40°C, because of the high Krafft point of CTABr. To investigate the effect of temperature on the phase boundaries, the following strategy was used. Selected samples situated close to the phase boundaries in the surfactant ion and polyion mixing planes were subjected both to heating to 50 °C in a thermoblock and to cooling to 8 °C in a refrigerator. Any changes in appearance (turbidity, birefringence) due to the temperature changes were noted. The results showed that the temperature effects in both phase diagrams were small. The only clear trend was found in the two-phase micellar regions in both mixing planes, where the two-phase region increased slightly in size on cooling.

Discussion

The Surfactant Ion Mixing Plane. One of the most striking findings of our study is the difference between the two surfactant ion mixing planes (Figures 3 and 4). These diagrams demonstrate that *changing the identity of the simple surfactant counterion* can lead to dramatic changes in the self-assembly and water solubility of an ionic surfactant with mixed polymeric and simple counterions. Note that only the left-most portions of the diagrams are the same. When the fraction of simple counterions is as low as 0.1, the two phase diagrams already differ widely: Bromide counterions give rise to a large area of micellar/hexagonal coexistence, whereas the latter two phases always are separated by a cubic phase in mixtures where acetate is the simple counterion.

The difference between the simple counterions may be ascribed to their effect on the curvature of the aggregate surface.

Bromide ions screen the headgroup repulsion more strongly, which leads to a lower aggregate curvature.[22,30] With bromide as the counterion, the micelles grow in size and form large rodlike aggregates, promoting a hexagonal phase. The acetate ion, on the other hand, gives a high curvature, which results in globular micelles. Consequently, CTAAc forms a cubic phase in water, whereas CTABr does not. As was noted previously,[22] polyacrylate is similar to acetate, in that it promotes a high curvature and small, discrete micelles of CTA^+ ions. Micellar cubic phases have, in fact, also been observed in covalent gels of polyacrylate with CTA^+ counterions.[11,12]

The difference in the *shape* of the surfactant aggregates can thus explain the structural differences of the phases found with bromide and acetate counterions. Similarly, the difference in the *size* of the surfactant aggregates would explain the difference in water solubility of the aggregates, when they have mixed polymeric and simple counterions. If the surfactant aggregates are large, only a small fraction of polyions is needed for phase separation, because there will be more polyions per aggregate and, hence, a stronger attraction per aggregate. This is shown by the large two-phase region and the narrow micellar region in the CTAPA/CTABr/H_2O system (see Figure 3). For small spherical micelles, on the other hand, a much larger fraction of polymeric counterions is required to induce phase separation (see Figure 4). When the aggregates are extended, the polyion-induced attraction is sufficient to crystallize the aggregates into a hexagonal phase with long-range order. For small spherical micelles, on the other hand, the initial phase separation, at the highest fractions of simple counterions, involves one concentrated and one dilute micellar solution, both belonging to the disordered micellar phase. Only when the fraction of polyions approaches unity is the attraction strong enough to crystallize the aggregates into a cubic phase.

Molecular Origin of Aggregate−Aggregate Interactions. Monte Carlo simulations provide further insight into the experimental phase diagrams. Figure 9 shows simulated force curves for planar or micellar aggregates with mixed monovalent/polymeric counterions. For both geometries, the forces switch from being purely repulsive at high fractions of monovalent counterions to being attractive at high fractions of polymeric counterions. A comparison between panels a and b in Figure 9 shows that the force acting between two planar aggregates is more attractive than the force between two spherical aggregates, and a lower fraction of polymeric counterions is required to obtain an attractive force between planar aggregates. This difference is qualitatively in agreement with the experimental observation that a smaller fraction of polyions is required to induce a phase separation for cylindrical aggregates than for spherical micelles.

To analyze the molecular origin of the force curves, it is instructive to partition the osmotic pressure (P_{osm}) into three components:

$$P_{osm} = P_{corr} + P_{bridge} + RTc(0) \qquad (3)$$

This form for the osmotic pressure comes from a consideration of the pressure acting across the midplane between the two charged surfaces. P_{corr} is the ion−ion correlation pressure, which is due to charges on either side of the midplane; this term is always attractive but vanishes in a mean-field approach. The bridging term, P_{bridge}, is due to polyion chains crossing the midplane. The last term in eq 3 is the standard entropic contribution. The correlation pressure is short-ranged and rather insensitive to the detailed structure of the counterions. Ion−ion correlations manifest themselves in two ways: they give rise to the P_{corr} term, but they also reduce the midplane concentration. The latter effect is often the most important one. Figure 10 demonstrates the relative importance of these three different pressure contributions for a planar system. One can note that a small fraction (one-sixth) of polymeric counterions gives rise to an attractive bridging component, but it is not strong enough to overcome the entropic repulsion. Note that the repulsive term is more long-ranged with a large fraction of monovalent counterions. When three-fourths of the monovalent counterions have been replaced by polymeric ions, a strong net attraction, which is due to the dominating bridging term, appears at a separation on the order of 10 Å.

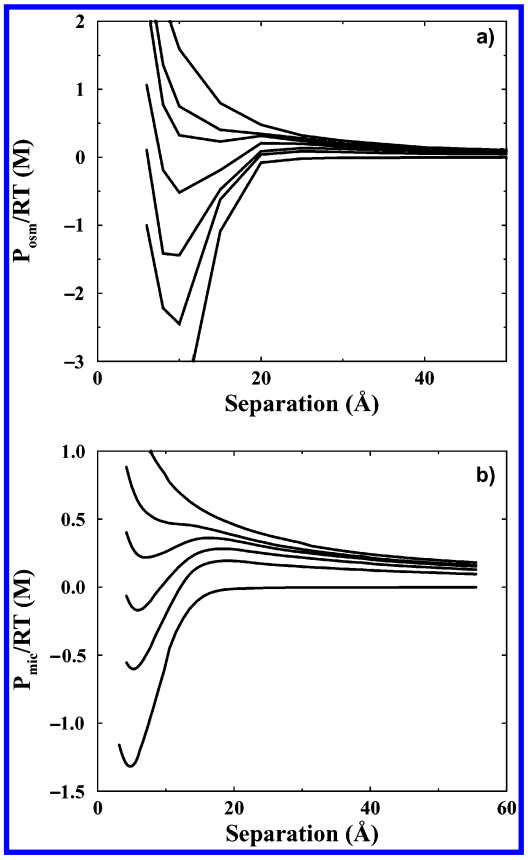

Figure 9. (a) Simulated osmotic pressure between two planar charged surfaces neutralized by a mixture of simple and polymeric counterions. The surface charge density is 0.13 C/m^2. From top to bottom, the fraction of simple ions is 1, 0.75, 0.58, 0.42, 0.25 and 0. (b) Pressure between two micelles (R = 24 Å), as obtained from panel a, using the Derjaguin approximation. The force has been divided by the micellar cross-sectional area, converting the force to a pressure. Notation is the same as that shown in panel a.

One may ask whether also the van der Waals attraction contributes significantly to the micelle−micelle attraction. However, this interaction is negligible in our systems. With a Hamaker constant of 0.5×10^{-20} J for the interaction of hydrocarbon across water, we find that the van der Waals interaction contributes <10% to the attraction in the minimum in Figure 9.

Tunable Interactions between Surfactant Micelles. We previously have seen that exchanging acetate counterions for polyacrylate counterions does not affect the shape or size of the surfactant aggregates; they remain small and discrete. In essence, the top portion of the CTAPA/CTAAc/H_2O phase diagram therefore describes the phase behavior of charged spheres with mixed polymeric and simple counterions. (Actually, the micelles of a *Pm*3*n* cubic phase are slightly, but significantly, elongated;[37] however, this should not affect the qualitative features that are

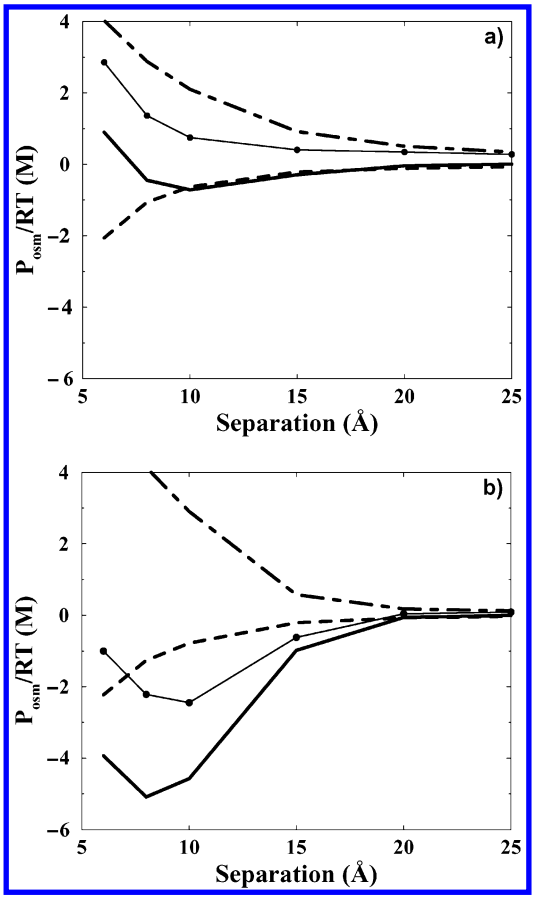

Figure 10. Decomposition (see text) of the simulated osmotic pressure between two planar charged surfaces with mixed simple and polymeric counterions. Parameters as shown in Figure 9a. The fraction of simple counterions is (a) 0.83 or (b) 0.25. Lines refer to the bridging term (solid line), the correlation term (dashed line), the entropic term (dot−dashed line), and the total osmotic pressure (thin line with symbols).

discussed in this section.) Changing the relative amounts of acetate or polyacrylate counterions is a way of tuning the sphere−sphere interactions.

Another way of tuning the interactions between colloidal particles in a solvent is by adding a soluble nonadsorbing polymer, which gives rise to a depletion attraction between the particles. The depth of the depletion attraction increases as the polymer concentration increases, whereas the range of the attraction is determined by the diameter of a polymer coil. Both theoretical[39,40] and experimental[41] work has shown that the phase diagrams of such colloid−polymer mixtures are quite analogous to the temperature−density phase diagrams of simple one-component fluids. Figure 11 reproduces theoretical phase diagrams for the latter type of system, where the particles interact via the Lennard-Jones $2n-n$ potential.[42] One particular feature of the phase diagrams for both simple fluids and colloid−polymer mixtures is that a stable gas−liquid critical point only exists for interactions that are sufficiently long-ranged, compared to the particle size, as has been shown in studies by Lekkerkerker and Poon and their co-workers.[41−43] For particles interacting via the Lennard-Jones $2n-n$ potential, the condition for stable gas−liquid coexistence is that $n \leq 11$.[42] For colloidal particles, the transition between the two types of phase diagrams in Figure 11 has been demonstrated experimentally by Ilett et al., who used polymers of different sizes to vary the range of the depletion attraction between spherical particles.[41]

In Figure 12, we explore the analogies between the CTAPA/CTAAc/H_2O phase diagram and the phase diagrams in Figure

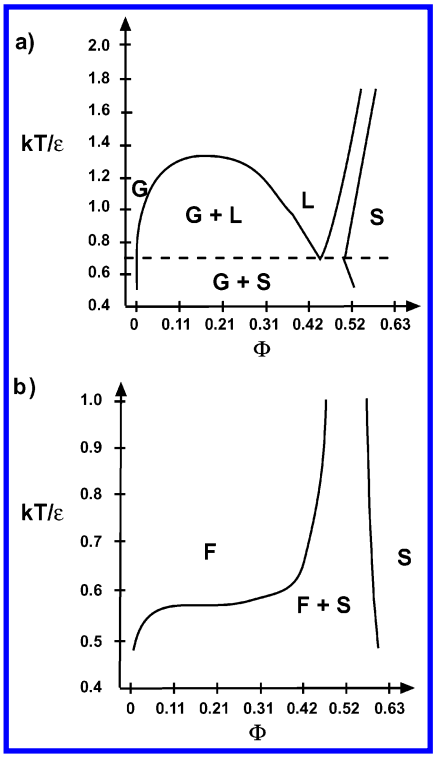

Figure 11. Temperature−density phase diagrams (redrawn from Vliegenthart et al.[42]) for particles interacting via a Lennard-Jones potential $V(r) = 4\epsilon[(\sigma/r)^{2n} - (\sigma/r)^n]$ with (a) $n = 6$ or (b) $n = 12$ (G = gas, L = liquid, S = solid, F = fluid).

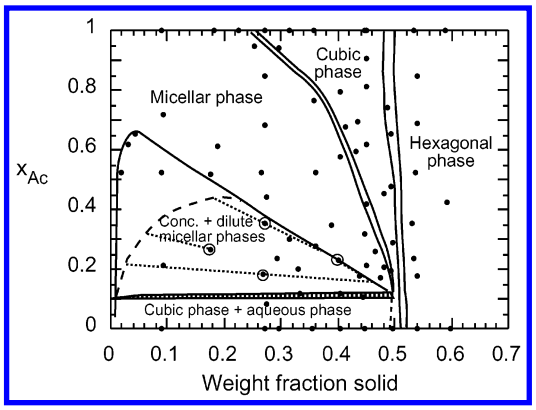

Figure 12. Mole fraction of acetate counterions, x_{Ac}, versus the weight fraction of solid in CTAPA/CTAAc/H_2O samples. Points represent the overall compositions of the samples. The plot is based on the same experimental data as the phase diagram in Figure 4. Tie lines are based on the results of the TGA analysis of the encircled samples (see Table 2). The dashed phase boundary of the two-phase micellar region line is the coexistence curve, connecting the end points of the tie lines.

11. To that end, we have redrawn the phase diagram in Figure 4, using the mass fraction of solid as the global concentration variable and x_{Ac} as the parameter controlling the interaction between the surfactant micelles. The parameter x_{Ac} in Figure 12 is analogous to temperature in Figure 11, in the sense that a decrease in x_{Ac} leads to an increasing dominance of the particle−particle attraction. Clearly, the main features of the diagram in Figure 11a are also present in Figure 12. At low x_{Ac} values, where the micelle−micelle attraction is strong, there is a coexistence between a "gas" phase and a "crystalline" (cubic) phase. As x_{Ac} is increased, a region of coexistence between the "gas" and "liquid" branches of the micellar phase is reached, via a narrow three-phase area. The dilute and concentated branches merge into a single fluid phase at sufficiently high

values of x_{Ac}. At high concentrations, irrespectively of x_{Ac}, the micelles crystallize into a cubic phase.

A comparison with the phase diagrams in Figure 11, and with similar phase diagrams for other interaction potentials,[39,40,44] suggests that the reason why there is a "gas−liquid" coexistence for CTA micelles with mixed polymeric and simple counterions is that the range of the attractive bridging interactions between the micelles is still sufficiently long-ranged, compared to the micelle diameter. Pursuing this analogy, we may suspect that sufficiently large charged spheres with mixed polymeric/monovalent counterions would display a phase diagram of the type shown in Figure 11b, displaying only liquid−solid coexistence.

Polydispersity Effects. Figure 12 shows two different experimental boundaries for the two-phase area of dilute−concentrated micellar coexistence. The inner boundary (dashed line) is a coexistence curve; this shows the equilibrium compositions (see Table 2) of macroscopically separated phases taken from the samples marked by circles in the figure. These samples were prepared far into the two-phase area and separated into two liquid phases of comparable volumes. The outer boundary (solid lines) is a cloud-point curve. This curve marks the boundary between samples that were found to be monophasic from those that were biphasic. Thus, the dilute samples located between the cloud-point curve and the coexistence curve in Figure 12 were found to be biphasic. Some actually contained a cubic phase in equilibrium with a dilute aqueous phases. These observations apparently violate the Gibbs phase rule. For a truly ternary system of the type depicted in Figure 12, the cloud-point curve and the coexistence curve must coincide. The discrepancy may be ascribed to the polydispersity of the polyion. Similar differences between cloud-point and coexistence curves are well-known for phase-separating polymer solutions containing polydisperse polymer components.[45] The difference between the cloud-point and coexistence curves is not evident in the representation in Figure 4; this is because, on the scale of the triangular phase diagram, the details of the dilute portion are not very well resolved.

Why Do Polyions Induce a Cubic-to-Micellar Phase Transition in CTAAc/H_2O? One striking feature of Figure 12 is that the location of the micellar-to-cubic phase transition varies quite strongly with x_{Ac}. This strong variation has no counterpart in the diagrams in Figure 11, and it also contrasts with the almost-vertical band of cubic−hexagonal coexistence in Figure 12. It seems interesting—also from a practical point of view—to understand why polymeric counterions "melt" the cubic phase so efficiently. Our studies show that the maximum concentration of the (pourable) micellar phase may be increased from 25 to 50 wt % by partially replacing the simple micellar counterions with polymeric counterions.

The interaction between micelles with only simple counterions is purely repulsive, because of the electrostatic double-layer repulsion. As the concentration of micelles is increased, the double-layer repulsion becomes stronger. Finally, it exceeds some critical value, where the system crystallizes. The fact that the crystallization occurs at a rather low volume fraction (ca. 0.25, compared to 0.494 for a system of hard spheres[46,47]) emphasizes the fact that it is the long-range electrostatic interaction, rather than the bare micellar radius, that gives rise to the repulsion. A naive explanation to the shrinking of the cubic phase with decreasing x_{Ac} would then be that the range of the micelle−micelle repulsion decreases when monovalent counterions are replaced by polymeric counterions. We have made some calculations to test this hypothesis. To compare this theory with the experimental variation, we need some criterion for when the repulsion is strong enough to induce crystallization. We have used the simple criterion that the micellar-to-cubic transition occurs at a constant osmotic pressure, P_{melt}, regardless of the counterion composition, because a constant osmotic pressure implies a constant force between the aggregates.[36] To obtain a value of P_{melt}, we used the cell model to calculate the osmotic pressure at the concentration where the micellar-to-cubic transition occurs in pure CTAAc.

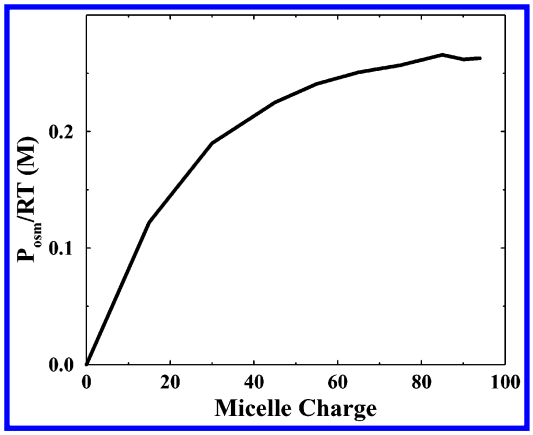

Figure 13. Simulated variation of the osmotic pressure, given by the cell boundary concentration of counterions, with micelle charge for a model spherical micelle neutralized by simple counterions only. The micelle radius was 24 Å, and the cell radius was 36.8 Å, corresponding to a volume fraction of micelles of 0.28.

A simple approach to the effect of polymeric counterions is to assume that every polyion condenses onto the micellar surface, so that each polyion charge effectively neutralizes one charge on the micellar surface. In this limit, the fraction of charged headgroups on the micelle is given by x_{Ac}. This reduces the osmotic pressure, and, to maintain a constant P_{melt}, the concentration of micelles must increase. Following this recipe, we calculated an isobaric line in the phase diagram in Figure 12 (not shown). This line correctly predicts a strong shrinking of the cubic phase as x_{Ac} varies from 1 to 0; however, the shape of the phase boundary is totally wrong. Although the experiments show a rapid variation at low fractions of polyions (x_{Ac} close to unity), the calculated boundary initially stays practically constant with decreasing x_{Ac}, and then varies increasingly more rapidly as the fraction of small counterions approaches zero. This is a consequence of the fact that P_{melt} is more or less independent of the surface charge density, after the latter is greater than a certain value. The latter phenomenon, which is well-known under the name of "counterion condensation" for highly charged linear polyelectrolytes, is illustrated in Figure 13 for model micelles.

It is thus clear that the strong effect on the phase boundary of a small fraction of polyions cannot be captured by the simple neutralization assumption. One obvious deficiency of the latter approach is that it completely neglects all bridging contributions (cf. Figure 10). To remedy this, we have also simulated a planar system with polyions and applied the Derjaguin approximation, as in Figure 9b. However, this causes only a slight change of the isobar, which is still very far from the experimental phase boundary.

In view of these simulation results, we must seek another reason why polyions melt the cubic phase so efficiently. We believe that this is due to the inherent heterogeneity of the system. The CTAPA/CTAAc/H_2O mixture contains finite micelles with a valency of ∼100 and polyions with a valency of ∼30. This means that if we replace, say, 1% of the monovalent

counterions with polyions, the effect is not smeared out uniformly on all micelles, because the number of micelles in such a mixture is 30 times larger than the number of polyions. Only a small fraction of micelles will contain one (or, rarely, more than one) polyion in their ionic atmosphere. For such a micelle, the local effect is large, because one polyion corresponds to 30% of its total counterion content. The majority of micelles will, however, still be surrounded by only monovalent counterions. Thus, we have a system that is necessarily inhomogeneous on a length scale much larger than the intermicellar distance. For the micellar phase, this inhomogeneity is directly evidenced by our SAXS spectra (Figure 7). This heterogeneity should strongly promote the destruction of long-range order, i.e., the melting of the crystalline (cubic) structure. Obviously, this heterogeneity cannot be captured by a simulation of an infinite planar system, where all polyion effects are averaged over the interacting surfaces.

Why Do Polyions Induce a Hexagonal-to-Micellar Phase Transition in CTABr/H_2O? Figure 3 shows that the transition from the micellar to the hexagonal phases in the system CTAPA/CTABr/H_2O is strongly affected by counterion composition at low polyacrylate contents: Small proportions of polyacrylate "melt" the hexagonal phase of CTABr in H_2O very efficiently, increasing the concentration range of the micellar phase. This effect is very similar to the effect of polyacrylate on the micellar-to-cubic phase transition of CTAAc, which we have just discussed. It would thus seem likely that the analogous effects in the two different systems have the same physical origin. Previously, we suggested that the melting of the hexagonal phase of CTABr by polyacrylate ions was due to an increased curvature of the micellar aggregates.[22] In light of the previous discussion, we now propose that the inhomogeneous distribution of polyions among the surfactant aggregates is the main reason why a small fraction of polyions melt the hexagonal phase of CTABr.

Why Do Polyions Have No Effect on the Cubic-to-Hexagonal Phase Transition in CTAAc/H_2O? Finally, we return to the CTAPA/CTAAc/H_2O system and discuss the insensitivity of the cubic-to-hexagonal phase transition to the counterion composition (Figures 4 and 12). This phase transition occurs at quite high surfactant concentrations. When the surfactant concentration in the cubic phase increases, the distance between the micelles decreases and the repulsion increases. At some point, the system may choose to decrease the repulsion by a change of structure, despite a possible increase in curvature free energy. The number of permitted structures is limited, because at least one dimension of the surfactant aggregate cannot be larger than twice the length of an extended surfactant molecule. Under these conditions, the system responds by switching to a hexagonal structure, because, at a constant volume fraction of aggregates with the same radius, the aggregate−aggregate distance is larger in a hexagonal structure than in a cubic structure.

The question remains as to why this transition is quite insensitive to polymerization of the counterions. Simulations show that, even in these highly concentrated systems, the force profiles are significantly different for polyvalent and monovalent counterions (see Figure 9). A simple isobaric criterion, as discussed previously, would therefore predict a significant slope of the phase boundary toward higher surfactant concentrations at lower x_{Ac}. It is, however, not obvious that we can apply this simple argument to the cubic−hexagonal transition, because the change in aggregate shape is accompanied by a change in surface charge density. It is likely that polymeric counterions screen the headgroup repulsion more efficiently than monovalent counterions, and this effect should favor the hexagonal phase, which has a higher charge density. Thus, we may have two compensating effects of polymeric counterions on the cubic−hexagonal transition.

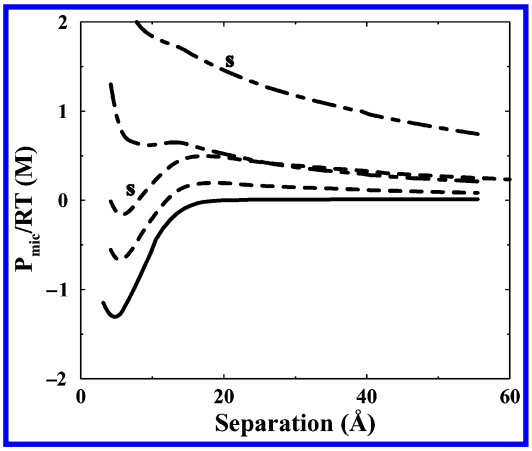

Figure 14. Simulated pressures between two micelles using the Derjaguin approximation. Solid curve represented micelles that have been neutralized by polymeric counterions only. The other curves refer to the same system with added excess electrolyte in the form of either polyelectrolyte or simple salt (marked "s"). The amount of added electrolyte, expressed in terms of the percentage of the micelle charges, was 8% (dashed curves) or 25% (dot−dashed curves).

In this context, we should also note that the simulations performed in this work are not expected to describe the phase diagram quantitatively—only qualitatively. The agreement could, of course, be improved by tuning certain input parameters in the simulation model; however, this would hardly lead to an improved understanding of the physical behavior.

The Polyion Mixing Plane. When NaPA is added to aqueous CTAPA, the solubility of the micelles is rapidly increased (Figure 8). This is similar to the effect that is observed when CTAAc is added (Figure 4), so one may ask whether the mechanisms for solubilization of the complex salt are the same in the surfactant ion and polyion mixing planes. From the surfactant-centered viewpoint, the answer is no (see Figure 2). When surfactant is added, the surfactant ions ultimately reside in the surfactant aggregates, and the counterions reside in the aqueous pseudophase. The result is colloidal aggregates that are neutralized by mixed polymeric and monovalent counterions. The solubility of such aggregates is determined by the polyion/simple ion mixing ratio, as we have observed previously. By contrast, when polyelectrolyte is added, both the polyions and its simple counterions are eventually considered to be excess electrolyte in the aqueous pseudophase. Therefore, the effect of added polyelectrolyte should be more similar to the effect of added simple salt. Our experiments showed, in fact, that the effects of these two different electrolyte additives were even quite similar quantitatively.

We have used computer simulations to investigate these similarities more closely. Figure 14 shows simulated force curves between micelles for various cases, representing the complex salt alone, or the complex salt with added excess simple salt, or polyelectrolyte. The amount of excess charge from the added salt is expressed in terms of the percentage of the charge of the complex salt. Figure 14 shows that, with only 8% excess electrolyte, both force curves show a minimum, meaning that these systems are expected to phase-separate. The curve for 25% added polyelectrolyte shows a weak local minimum and a local maximum. This system would thus be close to the critical point.

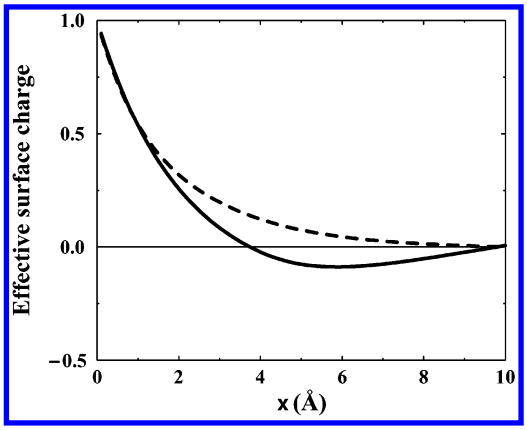

Figure 15. "Charge reversal" with added electrolyte. The simulated system is two infinite charged planes with neutralizing counterions and 25% excess electrolyte at a separation of 20 Å. The curves show how the effective surface charge density (see text) varies with the distance from the surface for simple counterions only (dashed curve), polymeric counterions only, or a mixture corresponding to exact neutralization by polymeric counterions + 25% added simple salt. The results for the last two cases superimpose (solid curve).

The curve for 25% added simple salt is monotonically decreasing at all separations but with a small oscillation in the derivative at close separations. Although there are quantitative differences between the force curves, the prediction is thus that the complex salt should dissolve with 25% excess polyelectrolyte, whereas the required excess of simple salt is somewhat less, but not much. This is in qualitative agreement with the experiments, although the quantitative discrepancy is considerable: The excess amount of electrolyte required for dissolution in the experiments is much higher (100%−200%) for both added salt or added polyelectrolyte. One factor that could contribute to this discrepancy is that the relative excess of salt can be different in the separating phases of the real system. This possibility is not captured by the simulations.

One simple-minded explanation of the effect of added excess polyelectrolyte would be that the excess polyions bind to the micelle surface, thereby giving rise to a reversal of the micelle charge. We could then imagine a repulsive system of "hairy", net negatively charged micelles with simple positive counterions. From the simulations, we can investigate the issue of charge reversal. We do this by defining the effective surface charge density, σ_{eff}, that is "seen" at some distance x from the surface as

$$\sigma_{\text{eff}} = \sigma_0 + \int_0^x \sum_i z_i c_i(x')\, \mathrm{d}x' \qquad (4)$$

Here, σ_0 is the surface charge density of the bare surface and $c_i(x)$ is the average concentration of ionic species i that carries the charge z_i a distance x from the surface. Figure 15 shows how the effective surface charge density varies with distance to the surface for the case of two charged planar surfaces separated by a 20 Å aqueous pseudophase containing neutralizing counterions and 25% added salt. All curves begin at the (normalized) surface charge density for $x = 0$ and, for symmetry reasons, they all end at zero effective charge at the midplane (x = 10 Å). For the case of simple ions only, σ_{eff} varies monotonically with distance between these endpoints. This type of system does not display a charge reversal. The other extreme case investigated is one where all the counterions are polyions; this corresponds to a mixture of complex salt plus a 25% excess of polyelectrolyte. In this case, a change in sign of σ_{eff} is observed for 4 Å < x < 10 Å. This means that, at these distances, the charge of the surface is overcompensated by the accumulated charge of all ions between the surface and the plane x. This effect is clearly compatible with the picture of a micelle with reversed charge due to the adsorption of an excess of polyions. Interestingly, however, virtually the same overcompensation, or charge reversal, is observed (Figure 15) in a system where the surfaces are exactly neutralized by polycounterions, and all excess electrolyte is in the form of simple salt. Here, the idea of a charge-reversed micelle is not so obvious, because there is no excess of polyions.

How can we understand this effect? First, we can realize that, when we replace polymeric counterions with monovalent counterions at a constant equivalent concentation, we must move gradually from one of the curves in Figure 15 to the other. In the case with neutralizing polycounterions plus 25% excess simple salt, most counterions are polyions, which is why the result is superimposed on that for only polyions. A more physical explanation of the results in Figure 15 is the following. If energy were to rule, the system considered would give rise to charge reversal in all cases. We then would have three layers of ions: one layer of counterions at some distance from either surface, and one layer of co-ions at the midplane. This electrostatic ordering is counteracted by entropy. With only small ions, entropy is strong enough to destroy the layering. However, when some, or all, of the counterions are polyions, the layering is retained, to some extent.

The conclusions from the analysis in Figure 15 may then be summarized as follows. (i) When simple salt or polyelectrolyte is added to the complex salt, similar effects are obtained, not only on the force curves but also on the charge distributions between the aggregates. (ii) As a corollary, we note that an explanation of the solubilizing effect of added polyelectrolyte, in terms of a charge reversal, considering merely the charge ratio between the polyions and the surfactant ions, is clearly too simplistic. This is shown by the fact that a similar charge reversal is obtained when only simple salt is added, keeping the polyion/surfactant ion charge ratio fixed at unity.

The final feature to discuss in the polyion mixing plane is that the cubic phase disappears when polyelectrolyte is added. Although we can offer no firm explanation for this effect, we can identify two possible mechanisms. The first is a simple dilution effect. All the added polyelectrolyte eventually resides in the aqueous subphase; therefore, the volume fraction of micelles decreases, which in itself would lead to a disappearance of the crystalline order. Second, the increased screening by the added polyelectrolyte should also decrease the surfactant headgroup repulsion, which could lead to micellar growth.

Conclusions and Outlook

In this work, we have used the simplest possible mixtures, with a reduced number of components, compared to conventional polyelectrolyte−surfactant mixtures, to study the factors that control the structure and water solubility of aggregates of oppositely charged polymers and surfactants. Clearly, this strategy should be useful also for other oppositely charged systems, such as polyion complexes or surfactant−polyion mixtures involving lamellar aggregates. Our study has led to the following conclusions.

The cetyltrimethylammonium (CTA^+) surfactant with mixed acetate and polyacrylate counterions provides a clean illustration of the effect of polymerizing the counterion, unobscured by ion-specific effects, on the phase behavior of its mixtures with water. The same types of aggregates and structures appear at all

counterion compositions. The surfactant aggregates remain small and essentially spherical, until a cubic-to-hexagonal phase transition occurs at high concentrations. The latter transition can be viewed as a way for the system to relieve the strong intermicellar repulsion that occurs at high concentrations of micelles.

The phase diagram for CTA^+ micelles with mixed polymeric and monomeric counterions shows that the micelle−micelle interaction changes from repulsive, when the simple counterions dominate, to strongly attractive, when the polymeric counterions dominate. This trend is supported by computer simulations, which also show that the dominating attractive term is polyion bridging. The resulting phase diagram is analogous to that of a hard-sphere colloidal dispersion in the presence of nonadsorbing polymers, where the depletion interaction may be used to tune the particle−particle interaction, or to the temperature−density phase diagram of an atomic one-component system.

The study confirms previous indications that the identity of the simple monovalent counterion may be quite important for the structure and solubility of surfactant aggregates with mixed polymeric and simple counterions. This is expected to be particularly relevant for cationic surfactants, where counterion-specific effects are strong. For the CTA^+ surfactant, even a small fraction of bromide ions induces aggregate growth. This affects the structure of the surfactant phases, and it also decreases the solubility of the surfactant aggregates in the presence of polymeric counterions.

Liquid crystalline phases of ionic surfactants (the cubic phase for cetyltrimethylammonium acetate and the hexagonal phase for cetyltrimethylammonium bromide) "melt" to disordered micellar phases when a small fraction of the monovalent counterions are replaced by polyions. This phenomenon occurs because the latter give rise to a strong perturbation of the aggregate−aggregate interactions and, thus, a heterogeneity of the system.

Our results immediately suggest several questions to be addressed by future research. How many charged units must a polyion contain to give a similarly strong attraction as observed here? What is the role of the charge separation along the polyion for the surfactant aggregate shape, and for the range of the aggregate−aggregate attraction? Is a liquid−liquid phase separation, induced by polyions, only observed for small colloidal aggregates? Why is the micellar cubic phase restricted to such a narrow concentration range when the counterions are polymeric? Work is in progress in our laboratory to answer these and similar questions.

Acknowledgment. This project used the X-ray beam of LURE and was funded by the Swedish SSF programme in Colloid and Interface Technology (A.S.) and the Swedish Research Council (L.P.). Håkan Wennerström and Ulf Olsson are acknowledged for valuable discussions.

References and Notes

(1) Goddard, E. D.; Anathapadmanabhan, K. P. *Interactions of Surfactants with Polymers and Proteins*; CRC Press: Boca Raton, FL, 1993.
(2) Kwak, J. C. T. *Polymer−Surfactant Systems*; Marcel Dekker: New York, 1998.
(3) Carnali, J. O. *Langmuir* **1993**, *9*, 2933.
(4) Chen, L.; Yu, S.; Kagami, Y.; Gong, J.; Osada, Y. *Macromolecules* **1998**, *31*, 787.
(5) Ilekti, P.; Piculell, L.; Tournilhac, F.; Cabane, B. *J. Phys. Chem. B* **1997**, *102*, 344.
(6) Ranganathan, S.; Kwak, J. C. T. *Langmuir* **1996**, *12*, 1381.
(7) Thalberg, K.; Lindman, B.; Karlström, G. *J. Phys. Chem.* **1991**, *95*, 6004.
(8) Wakita, M.-A.; Edwards, K. A.; Regen, S. L. *J. Am. Chem. Soc.* **1988**, *110*, 5221.
(9) Claesson, P. M.; Fielden, M. L.; Dedinaite, A.; Brown, W.; Fundin, J. *J. Phys. Chem. B* **1998**, *102*, 1270.
(10) Stubenrauch, C.; Albouy, P.-A.; Klitzing, R. V.; Langevin, D. *Langmuir* **2000**, *16*, 3206.
(11) Hansson, P. *Langmuir* **1998**, *14*, 4059.
(12) Hansson, P.; Schneider, S.; Lindman, B. *J. Phys. Chem. B* **2002**, *106*, 9777.
(13) Khandurina, Y. V.; Dembo, A. T.; Rogacheva, V. B.; Zezin, A. B.; Kabanov, V. A. *Polym. Sci.* **1994**, *36*, 189.
(14) Mironov, A. V.; Starodoubtsev, S. G.; Khokhlov, A. R.; Dembo, A. T.; Dembo, K. A. *J. Phys. Chem. B* **2001**, *105*, 5612.
(15) Sjöström, J.; Piculell, L. *Colloids Surf. A* **2001**, *183−185*, 429.
(16) Sokolov, E.; Yeh, F.; Khokhlov, A.; Grinberg, V. Y.; Chu, B. *J. Phys. Chem. B* **1998**, *102*, 7091.
(17) Zhou, S.; Yeh, F.; Burger, C.; Chu, B. *J. Polym. Sci. B* **1999**, *37*, 2165.
(18) Antonietti, M.; Conrad, J. *Angew. Chem., Int. Ed. Engl.* **1994**, *33*, 1869.
(19) Antonietti, M.; Conrad, J.; Thunemann, A. *Macromolecules* **1994**, *27*, 6007.
(20) Antonietti, M.; Maskos, M. *Macromolecules* **1996**, *29*, 4199.
(21) Claesson, P. M.; Bergström, M.; Dedinaite, A.; Kjellin, M.; Legrand, J.-F.; Grillo, I. *J. Phys. Chem. B* **2000**, *104*, 11689.
(22) Ilekti, P.; Martin, T.; Cabane, B.; Piculell, L. *J. Phys. Chem. B* **1999**, *103*, 9831.
(23) Kim, B.; Ishizawa, M.; Gong, J.; Osada, Y. *J. Polym. Sci. A* **1999**, *37*, 635.
(24) Kogej, K.; Evmeneko, G.; Theunissen, E.; Berghmans, H.; Reynaers, H. *Langmuir* **2001**, *17*, 3175.
(25) Merta, J.; Torkkeli, M.; Ikonen, T.; Serimaa, R.; Steniua, P. *Macromolecules* **2001**, *34*, 2937.
(26) Svensson, A.; Piculell, L.; Cabane, B.; Ilekti, P. *J. Phys. Chem. B* **2002**, *106*, 1013.
(27) Zhou, S.; Chou, B. *Adv. Mater.* **2000**, *12*, 545.
(28) Zhou, S.; Yeh, F.; Burger, C.; Chu, B. *J. Phys. Chem. B* **1999**, *103*, 2107.
(29) Linse, P.; Piculell, L.; Hansson, P. In *Polymer−Surfactant Systems*; Kwak, J. C. T., Ed.; Marcel Dekker: New York, 1998; Vol. 77, p 193.
(30) Hansson, P.; Jönsson, B.; Ström, C.; Söderman, O. *J. Phys. Chem. B* **2000**, *104*, 3496.
(31) Pashley, R. M.; McGuiggan, P. M.; Ninham, B. W.; Brady, J.; Evans, D. F. *J. Phys. Chem.* **1986**, *90*, 1637.
(32) Nydén, M.; Söderman, O. *Langmuir* **1995**, *11*, 1537.
(33) Morrison, R. T.; Boyd, R. N. *Organic Chemistry*, 4th Ed.; Allyn and Bacon, Inc.: Newton, MA, 1983.
(34) Metropolis, N. A.; Rosenbluth, A. W.; Rosenbluth, M. N.; Teller, A.; Teller, E. *J. Chem. Phys.* **1953**, *21*, 1087.
(35) Woodward, C. E.; Jönsson, B.; Åkesson, T. *J. Chem. Phys.* **1988**, *89*, 5145.
(36) Evans, D. F.; Wennerström, H. *The Colloidal Domain−Where Physics, Chemistry, Biology and Technology Meet*, 2nd ed.; John Wiley and Sons: New York, 1999.
(37) Fontell, K. *Colloid Polym. Sci.* **1990**, *268*, 264.
(38) Tanford, C. *The Hydrophobic Effect: Formation of Micelles and Biological Membranes*, 2nd ed.; John Wiley and Sons: New York, 1980.
(39) Gast, A. P.; Hall, C. K.; Russel, W. B. *J. Colloid Interface Sci.* **1983**, *96*, 251.
(40) Lekkerkerker, H. N. W.; Poon, W. C. K.; Pusey, P. N.; Stroobants, A.; Warren, P. B. *Europhys. Lett.* **1992**, *20*, 559.
(41) Ilett, S. M.; Orrock, A.; Poon, W. C. K.; Pusey, P. N. *Phys. Rev. E* **1995**, *51*, 1344.
(42) Vliegenthart, G. A.; Lodge, J. F. M.; Lekkerkerker, H. N. W. *Physica A* **1999**, *263*, 378.
(43) Lekkerkerker, H. N. W. *Physica A* **1997**, *244*, 227.
(44) Tejero, C. F.; Daanoun, A.; Lekkerkerker, H. N. W.; Baus, M. *Phys. Rev. E* **1995**, *51*, 558.
(45) Koningsveld, R.; Staverman, A. J. *J. Polym. Sci. C* **1967**, *16*, 1775.
(46) Pusey, P. N.; Megen, W. V. *Nature* **1986**, *320*, 340.
(47) Hoover, W. G.; Ree, F. H. *J. Chem. Phys.* **1968**, *49*, 3609.